IEEE Access
Multidisciplinary | Rapid Review | Open Access Journal

Received 21 May 2023, accepted 6 June 2023, date of publication 17 July 2023, date of current version 27 July 2023.

Digital Object Identifier 10.1109/ACCESS.2023.3296091

RESEARCH ARTICLE

Optimal Allocation of Curtailment Levels of PV Power Output in Different Regions in Consideration of Reduction of Aggregated Fluctuations

NOHA HARAG, CHIYORI T. URABE, (Member, IEEE), AND TAKEYOSHI KATO, (Member, IEEE)
Electrical Engineering Department, Nagoya University, Nagoya 466-0801, Japan

Corresponding author: Noha Harag (harag.noha.mamdouh.ali.hassan.w3@s.mail.nagoya-u.ac.jp)

This work was supported by the Ministry of Education, Culture, Sports, Science and Technology of Japanthrough providing MEXT scholarship funding.

ABSTRACT Due to the high penetration of photovoltaic power generation system (PV) anticipated in the future, the curtailment of PV power output becomes crucial, not only to maintain supply-demand balance but also to preserve an adequate capacity for the frequency control. When the curtailment level (CL) of the aggregated PV power output is determined in a day-ahead unit commitment (UC) scheduling, different CL should be applied to different regions with distinctive weather modes in the power system area so that the fluctuations of aggregated PV power output are minimized. The objective of this study is to optimally allocate the CL to each region based on the short-term forecasting of the weather modes so that the hourly maximum fluctuation of the aggregated PV power output (MF_{agg}) is minimized as long as the aggregated average power output (Avg_{agg}) becomes the same as the scheduled value in UC. Based on the past observations of PV power output, the proposed method employs relations between the regions' MF and CL (MF-CL patterns), and relations between the regions' Avg and CL (Avg-CL patterns) for several typical weather modes. Thus, a specific MF-CL pattern and Avg-CL pattern are determined for each region based on the short-term forecasting of the weather mode, and the CL optimization is proceeded by using these patterns. The proposed methods are tested by using the time-series of PV power output at 61 observation points in the central region of Japan for one year. As a result, it is demonstrated that merely acknowledging the weather mode of each region enabled the proposed methods to reduce MF_{agg} significantly and these results are practically similar to the method where perfect short-term forecasting of PV power output was utilized in the entire year.

INDEX TERMS Optimization, photovoltaic power, power curtailment, power fluctuations.

I. INTRODUCTION

Electric power systems are becoming increasingly vulnerable to system frequency fluctuations as renewable power generation gradually replaces conventional synchronous generation. A photovoltaic power generation system (PV) is one of the most promising renewable power generation due to its environment friendliness and abundance [1], [2], [3]. However, due to the nature of climate-driven PV power output fluctuations, it has been found that fluctuations of the high penetration PV power output not only induce significant voltage rise but also larger variation in frequency than ever. Therefore, the requirement for primary and secondary frequency regulation arising from significant real power imbalance on the grid side is increasing [4], [5].

The significant growth of PV capacity will lead electric power utilities to reinforce various ancillary services, such as frequency control. Several measures have been taken to mitigate this intermittent behavior associated with high PV penetration in order to maintain the supply-demand balance.

The associate editor coordinating the review of this manuscript and approving it for publication was Youngjin Kim.

These measures include proactive curtailment of PV power output, battery energy storage, and demand response along with leveraging spatial diversity by distributing PV across a large geographical area. While the implementation costs of energy storage systems are undoubtedly high [6], [7], [8], curtailment remains a cost-effective and conventional technique, involving the deliberate reduction in power output to balance power supply and demand [9], [10], [11], [12], [13].

PV power curtailment can serve as an important tool for operational planning, enabling power system operators to manage the variability of PV power generation. For instance, if the power output of PV and other generation resources exceeds the amount required to meet demand, the system operator may need to curtail the output of some PVs in consideration to the flexibility requirement [14]. In Japan, PV power output curtailment has been already implemented for few years in the Kyushu region, which has a high concentration of PV installations. Currently, power curtailment actions are expanding to other regions with high electricity demand such as the central region. Japan's current PV capacity is approximately 70 GW while the target capacity is anticipated to be 300 GW in 2050. Therefore, the entire electric power companies of Japan will consider PV power output curtailment in the coming years [15].

The curtailment will be implemented by using a smart inverter based on the request of the system operator. Since, the curtailment can preserve a control margin of PV power output, a smart inverter can use this margin further to provide the frequency control. This means that a smart inverter can have the ability of further suppressing or eliminating the frequency fluctuations. The effectiveness of smart inverters in suppressing the frequency fluctuations is demonstrated through advanced control strategies that significantly reduce the variability and uncertainty of PV power output, ultimately improving grid stability [16].

However, severe curtailment of PV power output should be reduced as much as possible because it is a significant waste of clean energy. One of the reason for curtailment is to preserve the required capacity for frequency regulation. Therefore, it is essential to determine the curtailment level (CL) of each PV power output to minimize fluctuations in the aggregated PV power output which is a major cause of frequency fluctuations. By reducing the required capacity, the need for curtailment can be reduced, thereby mitigating the waste of PV power output.

In a day-ahead unit commitment (UC) scheduling of required generation resources based on a day-ahead forecast of electricity demand and various renewable power generation, the CL of the aggregated PV power output is determined [17], [18], [19]. The curtailed PV power output helps maintain the supply-demand balance of the power system and provides adequate capacity for the frequency control [20], [21]. In the current UC scheduling, the CL of the aggregated PV power output is determined without considering the distinct fluctuating behavior of each region within the power system service area. However, different CL among each region should be applied to reduce the fluctuations in the aggregated PV power output. This will contribute to maintaining the frequency variations within the acceptable ranges determined by the grid codes, reducing the requirement of frequency regulation. Therefore, the main objective of this study is to propose an optimal allocation of CL among each region. In achieving this, accurate forecasting of power output fluctuation characteristics, as well as the average power output, is essential.

Numerous studies have been conducted on day-ahead forecasting PV power output from various perspectives, including statistical, mathematical, physical, machine learning, and hybrid forecasting models [22], [23], [24], [25], [26], [27]. As PV penetration increases, the short-term forecasting becomes crucial to ensure the attainment of the required PV power output for each hour on the operation day. Highly accurate short-term forecasting enables further adjustment of CL compared to the pre-determined CL by the UC scheduling. Currently, forecasting the average value of PV power output in short-term, ranging from few minutes to few hours, is feasible and different methods are discussed in [28]. These methods can be broadly divided into physical and data-driven approaches. In [29], a data-driven using neural network models and deep learning technology was employed to predict the short-term average value of PV power output with a high level of accuracy. On the other hand, the forecasting of short-term fluctuations of PV power output still remains challenging, with a considerable amount of error even when using machine learning algorithms and other advanced modeling techniques [30], [31], [32], [33], [34]. Therefore, this study tackles this issue through a more straightforward novel approach assuming that the fluctuation characteristics can be predicted in the short-term forecasting and be expressed in several typical patterns.

The main contributions of this study is firstly the formation of statistical relations of average value and maximum fluctuation against different CL, respectively. These relations are used to distinguish each region PV power output behavior in short-term. Secondly, using these relations, this study proposes an optimization of different CL to be allocated to each region. In this approach, the optimal CL in each region will minimize the fluctuation of aggregated PV power output without precisely forecasting the time-series of PV power output. As a result, the proposed method can contribute to the reduction of the control burden needed to eliminate the frequency fluctuations, thereby reducing the required resources for frequency control or secondary control in the power system.

This paper is divided into the following sections. Section II describes the irradiance data used in this study. Section III discusses the concept of five different methods of CL adjustment together with three methods for comparison. Section IV demonstrates an example used to show the procedure of data preparation and calculation process for the proposed methods of CL adjustment. Using the example of Section IV, Section V represents the application of all the adjustment

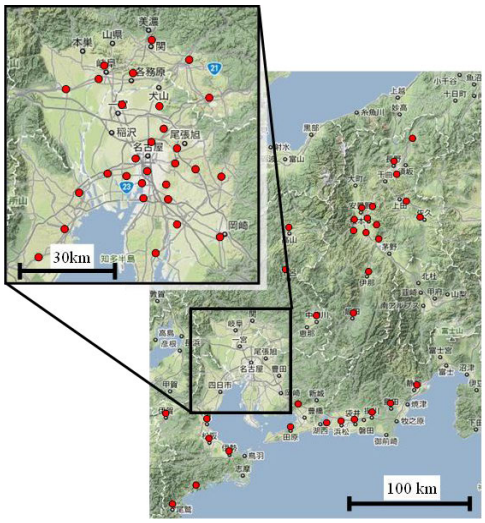

FIGURE 1. Location of multi observation points of PV power output in Chubu region, Japan.

methods on the day of operation. Finally, Section VI is dedicated to the results and discussion of the application of all methods over an entire year data.

II. DATA UNDER INVESTIGATION

Although the numbers of PVs are installed in each region of the power system service area, the availability of time-series data for PV power output or irradiance at a fine temporal resolution is limited to specific sites in each region. To estimate the aggregated power output data observed at these limited locations, a low-pass filter (LPF) model can be utilized [35]. The LPF model incorporates a smoothing effect that considers the geographical size of each representative region, resulting in reduced fluctuations in the aggregated power output compared to those at individual points.

In this study, the aggregated PV power output is calculated using the irradiance data observed at 61 points shown in Fig. 1. The 61 observation points are evenly distributed in the central region of Japan which is called Chubu region according to the population distribution, except for Nagoya City that is enlarged in Fig. 1. The distance between each pair of the neighboring observation points varies between 4.2 km and 138 km, and the average distance is 22 km. The 61 representative regions of each observation point is determined using Voronoi decomposition [35].

The irradiance data used in this study are observed from September 2010 to August 2011, which equals to 363 days. These data have a fine temporal resolution of one minute for an entire year. As these data are obtained from 61 points in one specific region in Japan, it is considered to be an advantageous point of this study.

The aggregated time-series data of curtailed PV power output for a certain period, is denoted as $P_{agg}^{CL}(t)$, is expressed as the weighted sum of PV power output of each region after applying curtailment, as shown in (1).

$$P_{agg}^{CL}(t) = \sum_{i=1}^{61} \omega_i P_i^{CL}(t) = \sum_{i=1}^{61} \omega_i \frac{I_i(t)}{I_{max}} CL_i \tag{1}$$

where, $P_i^{CL}(t)$ is the time series curtailed PV power output for individual region i, ω_i is the weighted factor based on each region's installed capacity, $I_i(t)$ is the time series irradiance of each region, I_{max} is the maximum irradiance, thus 1000 W/m^2, and CL_i is the curtailment level applied for each region. Because ω_i is determined in consideration to the aggregated capacity of PV in the power system service area, P_{agg}^{CL} and P_i^{CL} are expressed in per unit (p.u.).

Considering that the curtailment will be applied when PV power output is high usually in the period from 10:00 to 14:00, the proposed methods are tested for one hour from 12:00 to 13:00 for the entire days of the year. This particular hour provides a reasonable representation to the diverse PV power output behaviors exhibited by the 61 regions for every day across different seasons. For instance, in Japan, the temporal resolution of irradiance forecasts is one hour. Even within a one-hour time horizon, variability and uncertainty of PV power output persist. For example, within this hour, some days may show high average PV power output and low fluctuations during the summer season, while other days may exhibit low average PV power output and low fluctuations in few days in winter. Spring and autumn days may display a wide range of both low average PV power output and fluctuations. Therefore, analyzing the performance of proposed method using one-hour time window allows for meaningful statistical analysis, even without using longer period for each day. The following sections will demonstrate the different methods of CL adjustment.

III. CL ADJUSTMENT METHODS

The unit commitment scheduling is conducted a day-ahead to determine the supply requirements of different generation resources based on the forecasted demand for the next day. In the current day-ahead UC scheduling, the CL of the aggregated PV power output is determined regardless of the distinctive fluctuating behavior of each region in the power system service area. However, different CL among each region should be applied to reduce the fluctuations in the aggregated PV power output. Therefore, as explained below, the proposed methods further adjust the CL in the real-time operation of the day based on the short-term forecasting of PV power output in each region.

A. PROPOSED CL ADJUSTMENT METHODS

1) SHORT-TERM ADJUSTMENT OF CL BASED ON SHORT-TERM FORECASTING OF HOURLY AVERAGE OUTPUT (METHOD-1)

The main purpose of CL adjustment in Method-1 is to achieve the hourly average value of resultant P_{agg}^{CL}, which is referred to

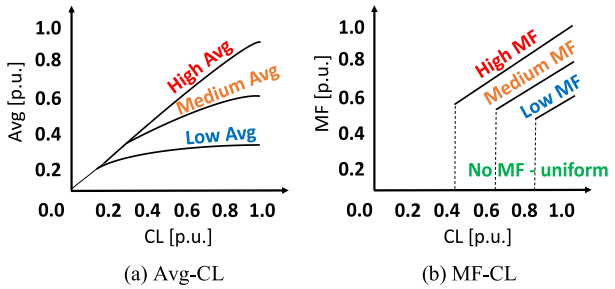

(a) Avg-CL (b) MF-CL

FIGURE 2. Concept of hourly average and maximum fluctuation of PV power output as a function of CL.

as Avg_{agg}^{CL}, equal to the predetermined average by the system operator (Avg_{pre}) in the short-term. Although Method-1 is not intended to reduce the fluctuations of the aggregated PV power output, Method-2, which is the main proposal in this study, is developed based on Method-1. Therefore, Method-1 is explained as a part of proposed method. Avg_{agg}^{CL} is simply defined in (2) where T is 60 minutes.

$$Avg_{agg}^{CL} = \frac{1}{T}\sum_{t=0}^{59} P_{agg}^{CL}(t) \tag{2}$$

Considering the fluctuations within one hour, the Avg_{agg}^{CL} is not a simple linear function of CL. Therefore, in the proposed Method-1, when short-term (i.e. few hours ahead) forecasting of PV power output in each region takes place, the adjusted CL is allocated to each region distinctively based on the relation between CL and the corresponding hourly average curtailed PV power output for each region (Avg_i^{CL}) where Avg_i^{CL} is simply defined in (3). The relations between Avg_i^{CL} and CL are called Avg-CL patterns and the concept of these patterns is shown in Fig. 2(a).

$$Avg_i^{CL} = \frac{1}{T}\sum_{t=0}^{59} P_i^{CL}(t) \tag{3}$$

The Avg-CL patterns are prepared based on the analysis of the observed PV power output in the past. The three patterns of Avg-CL can be expressed to range from high Avg to low Avg modes. Thus, instead of exact Avg_i^{CL} forecasting, the prediction of the mode to which the value can be categorized is enough for the proposed method. By predicting Avg mode, CL is adjusted and the Avg_{agg}^{CL} can be more accurate compared to the Avg_{pre} determined a day-ahead.

It is noted that Method-1 indirectly gives an insight into the characteristics of PV power output fluctuations. For instance, the medium Avg mode reflects the case when fluctuations are high at either low or high PV power output. Therefore, to precisely adjust CL, more information about the fluctuations becomes crucial and hence the next method is proposed. Fig. 3 includes the CL adjustment procedures of Method-1 in blue. They are composed of two main steps: preparation of Avg-CL patterns in Section IV, and the utilization of these patterns to apply CL adjustment methods on the day of operation in Section V.

2) SHORT-TERM ADJUSTMENT OF CL BASED ON SHORT-TERM FORECASTING OF HOURLY AVERAGE OUTPUT AND FLUCTUATIONS (METHOD-2)

The main purpose of CL adjustment in Method-2 is to minimize the maximum fluctuations of the aggregated PV power output (MF_{agg}^{CL}) as long as the predetermined Avg_{pre} is met. CL adjustment in this method undergoes a more advanced approach than Method-1 by considering the PV power output fluctuations directly. Despite the fact that the forecasting of actual fluctuations is challenging, the forecasting of typical fluctuation patterns can be available.

The relations between hourly maximum fluctuations of PV power output for each region MF_i^{CL} and CL are called MF-CL patterns and the concept of these patterns is shown in Fig. 2(b). They are also prepared for typical four PV power output characteristics based on the analysis of the observed PV power output in the past. The four patterns of MF-CL can be expressed to range from high MF to no MF (i.e. uniform output) modes. Thus, instead of forecasting the exact MF_i^{CL} and Avg_i^{CL}, the prediction of the modes to which these values can be categorized are needed. By predicting the PV power output behavior (i.e Avg and MF modes), CL is adjusted and the resultant Avg_{agg}^{CL} can even be closer to the Avg_{pre}. The short-term forecasting of Avg modes and MF modes are addressing a simple categorization of the regions from high Avg to low Avg modes and high MF to no MF. The entire Fig. 3 shows the two main steps of preparation of Avg-CL and MF-CL in Section IV, and the utilization of both Avg-CL and MF-CL patterns to apply the CL adjustment methods on the day of operation in Section V.

B. COMPARATIVE CL SETTING METHODS

1) NO CURTAILMENT (METHOD-0)

Method-0 represents the case when no curtailment is enforced. This is when the entire PV power output is used to balance out the demand along with other generation resources. Whereas frequency regulation can be achieved effectively by mechanisms such as battery energy storage and demand response, without any requirement for PV power curtailment.

2) SAME CL FOR ALL REGIONS (METHOD-3)

When the curtailment of PV power output is requested by the current UC scheduling a day-ahead, it merely applies the same CL to all the regions in the power system regardless of each region's behavior of PV power output for each hour on the next day, and no adjustment of CL is applied. Consequently, this might lead to unsatisfying the Avg_{pre} scheduled by the UC to meet the demand especially when the PV power output is fluctuating. This method can be efficient in situations where the PV power output is uniform only.

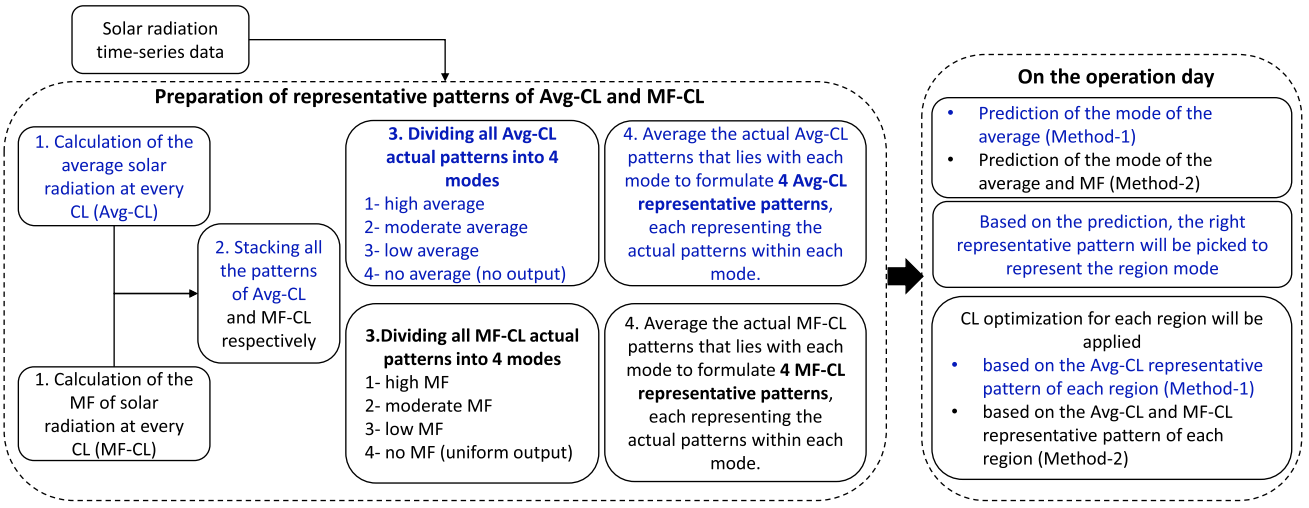

FIGURE 3. High level schematic of the procedures of the preparation of data and usage of the data on the operation day for the proposed methods of CL adjustment.

3) SHORT-TERM ADJUSTMENT OF CL BASED ON PERFECT FORECASTING OF AVERAGE AND FLUCTUATIONS (METHOD-4)

In Method-2, short-term forecasting of Avg modes and MF modes are addressing a simple categorization of the weather mode of each region. In Method-4, it is assumed that the perfect short-term forecasting of the time-series of PV power output in each region is available. This kind of zero-error forecasting is challenging and nearly impossible. Therefore, Method-4 is assumed to be an ideal situation and merely used for comparison with the proposed methods.

IV. DATA PREPARATION FOR THE REPRESENTATIVE AVG-CL PATTERNS AND MF-CL PATTERNS

The data preparation procedure of the proposed methods is applied to the 61 regions for every hour in each month. As an example, this section shows the data preparation of the representative patterns for one hour (from 12:00 to 13:00) in September. In each step, an example of four regions was used to demonstrate the concept and calculation output in each method. Fig. 4(a) shows the raw PV power output time-series data of the four regions on 1st September and their Avg_{agg}^{CL}. The different PV power output behaviors of the four regions for corresponding weather modes are identified as the following:

- Region (R) 1 has a high Avg and moderate MF.
- R11 has a high Avg and no MF, i.e. uniform PV power output.
- R29 has a moderate Avg and low MF.
- R51 has a low Avg and high MF.

A. METHOD-1

Step 1: Application of LPF to past measured PV power output time-series data.

As described in Section II, each of the 61 points represents the spatial average PV power output in each of the 61 regions.

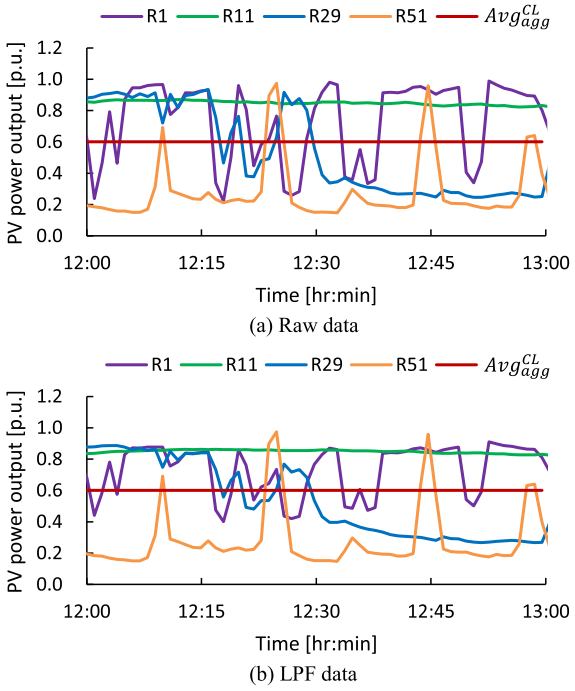

FIGURE 4. PV power output of the 4 regions on the 1st September.

In Fig. 4(b) the filtered PV power output data of the four regions on 1st September and their Avg_{agg}^{CL} are also shown. The filter gain of the LPF depends on the area of each region, i.e. the smaller the area, the smaller the filter gain applied and hence less reduction of fluctuations is witnessed. As R51 is a region with small area, the raw data and LPF data in Fig. 4(a) and Fig. 4(b) are almost similar.

Step 2: Application of different CL.

For the 61 regions, different CL are applied on their observed time-series PV power output data ranging from 0 to 1.0 p.u. with an increment of 0.01 p.u.

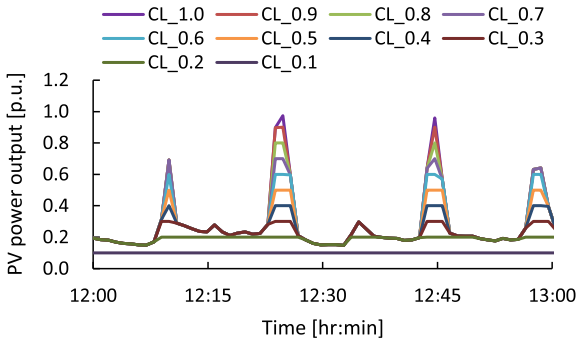

FIGURE 5. Different CL applied on R51 data on 1st September.

No curtailment is applied at 1.0 p.u. level, and 100% of curtailment is applied at 0 p.u. level. Fig. 5 shows an example of this step using the time-series data of R51 with an increment of 0.1 p.u. only.

Step 3: Computation of Avg_i^{CL} for each region.

The Avg_i^{CL} will be computed at each CL for every hour of interest at every day of the month. The actual Avg-CL patterns for 61 regions at one hour (here, from 12:00 to 13:00) for the entire days of September are plotted in Fig. 6(a). The actual Avg-CL patterns of the four regions on 1st September are shown separately in Fig. 6(b).

Step 4: Formation of the representative patterns of Avg-CL.

The Avg-CL patterns of the 61 regions for 30 days for one hour are stacked. Fig. 6(a) shows the Avg-CL patterns (1,830 patterns) of the 30 days of September for one hour (from 12:00 to 13:00). The maximum and minimum Avg-CL patterns are detected, then, all the patterns that lie within them are divided into three equal parts horizontally. These parts represent three modes; mode 1, mode 2 and mode 3 indicate low Avg, moderate Avg, and high Avg, respectively. The patterns that lie in each mode are averaged to get a single representative Avg-CL pattern for each mode, as shown in Fig. 6(c). Fig. 6(c) is shown as a dotted line as it reflects a prepared table of representative values of Avg against each increment of CL.

Since predicting the actual pattern of Avg-CL for the next hours can be challenging, then by just acknowledging the behavior of PV power output for the next hour, the Avg-CL representative patterns of Fig. 6(c) can be used instead of the actual patterns in Fig. 6(a). After that, optimization will be operated using these Avg-CL representative patterns. As shown in Fig. 6(c), it is difficult to express the relation between Avg and CL by using a simple function. Therefore, as described below, the optimization problem is formulated with a mixed-integer linear programming (MILP) by preparing a look-up table regarding the relation between Avg and CL. Therefore, in Fig. 6(c), plots showing the relation between Avg and CL are used instead of lines used in Figs. 6(a) and 6(b)

B. METHOD-2

Step 1: Application of LPF to past measured PV power output time-series data.

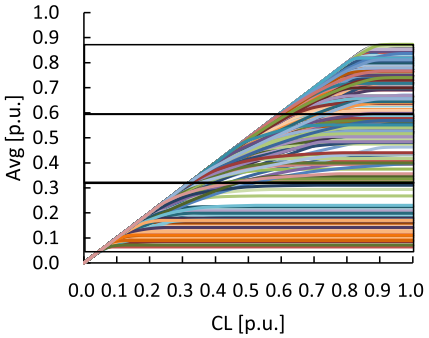

(a) The stacking of the actual patterns of the 61 regions for the entire month of September

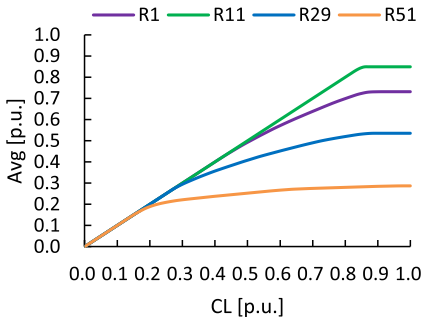

(b) The actual patterns of the four regions only on 1st September

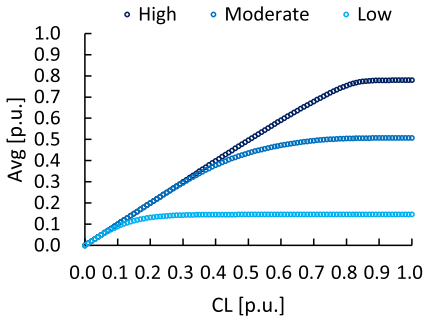

(c) The representative patterns used for 61 regions from 12:00 to 13:00 for the month of September

FIGURE 6. Avg-CL patterns.

The procedure in this step is the same as that in Method-1 described above.

Step 2: Application of different CL.

The procedure in this step is the same as that in Method-1 described above.

Step 3: Application of high-pass filter (HPF) on every curtailed PV power output data.

HPF function with a cut-off frequency of 32 minutes is applied to the time-series data calculated in steps 1 and 2. This is implemented to highlight the fluctuations and hence, maximum fluctuation of the HPF data will be calculated in the next step. Fig. 7 shows an example of the HPF data applied on the curtailed data of R51 on 1st September.

Step 4: Computation of MF_i^{CL} using the HPF data of each region based on a few parameters.

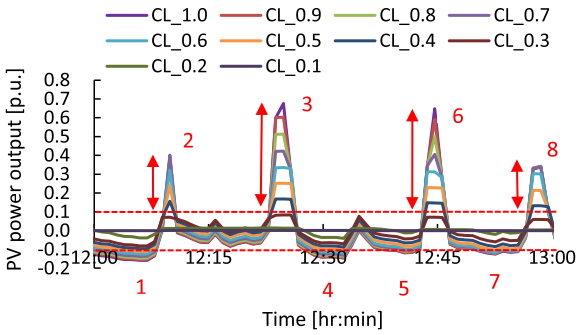

FIGURE 7. Application of HPF to different curtailed PV power data of R51 on 1st September.

The MF is the difference between the maximum and minimum points of fluctuations calculated in 20-minute-moving-window, and this parameter represents the short-cycle fluctuation in the time-series data. It varies with days and is independent of the season, because the movement of clouds is the reason for the short-cycle fluctuations.

To consider whether a region's PV power output behavior is fluctuating or not, this study sets some parameters to distinguish the fluctuating behavior such as threshold, count and range. Firstly, the threshold is an initially assumed value of PV power output. When the fluctuations cross this value for a number of times (count) shown in Fig. 7, they get recorded. In addition, the range is the sum of the heights of crossing fluctuations shown by the red arrows in Fig. 7. Crossings can be frequent as it can be very short in terms of power changes, then the sum of the heights of crossings becomes a crucial parameter and it gets recorded instead. The total number of times the threshold is passed and the sum of heights of these crossings contain essential information to capture the fluctuations.

When the PV power output changes comply with the pre-set number of count and range, it is characterized as fluctuating. Consequently, MF_i^{CL} is calculated and plotted against each corresponding CL. When the threshold is 0.1 p.u., count is 3, and range is 0.1 p.u., the MF_i^{CL} for the 61 regions at every CL is plotted in Fig. 8(a). The actual MF-CL patterns of the four regions on 1st September are shown separately in Fig. 8(b).

Step 5: Formation of representative patterns of MF-CL.

The MF-CL patterns of the 61 regions for 30 days for one hour are stacked. Fig. 8(a) shows the MF-CL patterns (1,830 patterns) of the 30 days of September for one hour (from 12:00 to 13:00). The maximum and minimum start of MF-CL patterns are detected, then, all the patterns that lie within them are divided into three equal parts vertically. These parts represent three modes; mode 1, mode 2, and mode 3 indicate low fluctuations, moderate fluctuations, and high fluctuations, respectively. While, mode 0 is representing regions with no fluctuations (uniform output). We average the patterns that lie in each mode to get a single representative MF-CL pattern for each mode as shown in Fig. 8(c).

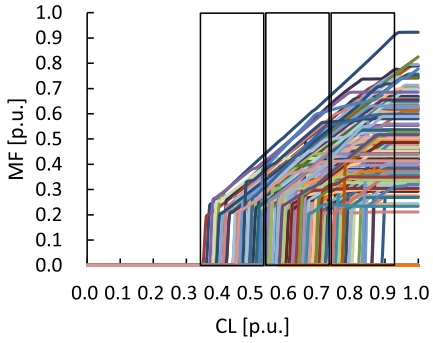

(a) The stacking of the actual patterns of the 61 regions for the entire month of September

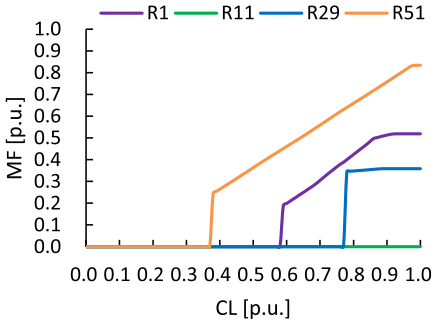

(b) The actual patterns of the four regions only on 1st September

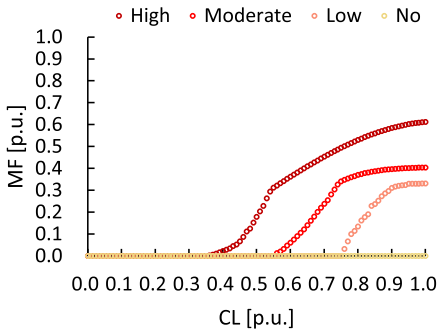

(c) The representative patterns used for 61 regions from 12:00 to 13:00 for the month of September

FIGURE 8. MF-CL patterns.

Fig. 8(c) is shown as a dotted line as it reflects a prepared table of representative values of MF against each increment of CL.

Since predicting the actual pattern of fluctuation for the next hours can be challenging, then by just acknowledging the characteristics of fluctuations for the next hour, the MF-CL representative pattern of Fig. 8(c) can be used instead of the actual pattern in Fig. 8(a). After that, optimization will be operated using these representative patterns. As mentioned below, the proposed optimization method is formulated with MILP in consideration of complicated relation between MF and CL. In Fig. 8(c), therefore, plots are used instead of lines as in Fig. 8(a) and (b) due to the same reason for Fig. 6(c) so as to show the discrete relation between MF and CL.

V. APPLICATION OF CL ADJUSTMENT METHODS IN THE ACTUAL OPERATION PERIOD

A. PROPOSED CL ADJUSTMENT METHODS

1) METHOD-1

The distinctive representative Avg-CL patterns for each region are used for the actual operation period. Hence, the CL will be optimized among each region so that Avg_{agg}^{CL} equals to the predetermined average by the system operator. For practical application, discrete values of CL are applied as the values of Avg_i^{CL} and MF_i^{CL} corresponding to CL in Figs. 6(c) and 8(c) are also discrete. The MILP problem is expressed in (4) to (8) where the objective is to minimize the gap between the Avg_{pre} and resultant Avg_{agg}^{CL} per hour. Although any kinds of solver for MILP problem can be used, in this study, the optimization process is operated by MATLAB Intlinprog function.

$$\min \left| Avg_{pre} - Avg_{agg}^{CL} \right| \tag{4}$$

It is formulated into linear optimization equations:

$$\min \; Avg_{pre} - Avg_{agg}^{CL} \tag{5a}$$

$$\min \; Avg_{agg}^{CL} - Avg_{pre} \tag{5b}$$

$$\text{i.e.} \quad Avg_{pre} = constant \tag{6}$$

$$Avg_{agg}^{CL} = \sum_{i=1}^{61} \sum_{k=0}^{100} n_i^k \omega_i Avg_i^k \tag{7}$$

$$\text{Subject to} \sum_{k=0}^{100} n_i^k = 1, \quad n_i^k \in \{0, 1\} \tag{8}$$

In the proposed method, one of the Avg-CL pattern is selected based on the short-term forecasting of weather mode for each region i. Therefore, $Avg_i^k (k = 0 - 100)$ in (7) corresponds to individual plots of the selected Avg-CL pattern. The number of possible CL applied is referred to as k and there are 101 candidates ranging from 0 to 1.0 p.u. with an increment of 0.01 p.u. By using the constraint in (8), one of the k values is selected and hence Avg_i^k is selected among the 101 candidates. In (7) and (8), n is a decision variable. The lower bound of n is 0 meaning that one of the possible CL is not selected and the upper bound is 1 meaning that one the possible CL is selected. At every iteration for each region, only one CL is chosen to be 1 leaving the other possible CL with 0. Hence, the sum of the decisions will always be 1.

For the four regions, R1, R11, R29 and R51, the short-term forecast of Avg-CL patterns from 12:00 to 13:00 on 1st September provides information that R1 and R11 have a high Avg, R29 has a moderate Avg and R51 has a low Avg. Hence, they are given the corresponding representative Avg-CL patterns that were prepared previously in Fig. 6(c).

As a result of the optimization assuming Avg_{pre} value of 0.5 p.u., Fig. 9(a) shows CL allocated on the four regions where R1 and R11 of the high Avg had the highest CL while R29 and R51 of lower Avg had lower CL. The resultant Avg_{agg}^{CL} is 0.54 p.u. and it is close to the Avg_{pre}.

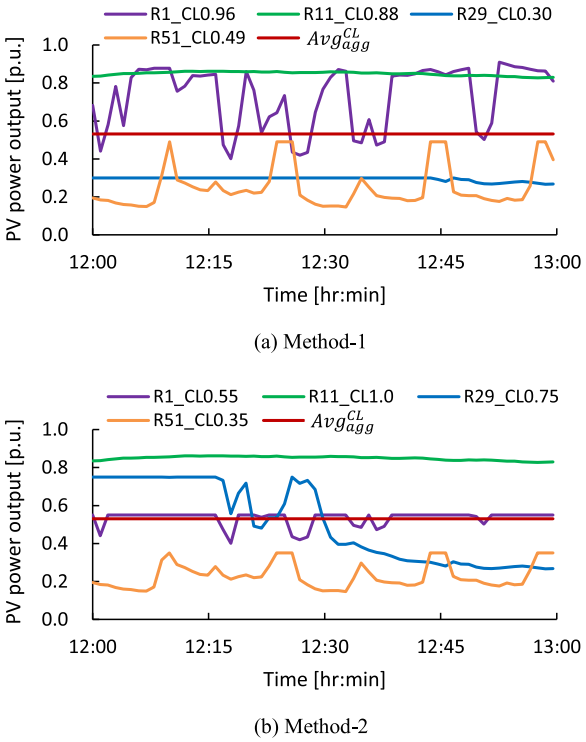

FIGURE 9. Application of the proposed CL adjustment methods.

2) METHOD-2

Both the distinctive patterns of MF-CL and Avg-CL for each region are used for the actual operation period, and the CL is optimized among each region. The optimization objective is to minimize the MF_{agg}^{CL} based on the different candidates of allocated CL as long as the Avg_{pre} is achieved. A buffer of 0.01 p.u. is added to the Avg_{pre} as CL are applied at an increment of 0.01 p.u. In this step, the optimization problem is also a MILP problem and it is shown in (9) to (11) to minimize the MF_{agg}^{CL}. MF_{agg}^{CL} is expressed as the root mean square (RMS) of MF of each region per hour. The RMS value is used in this optimization as the MF_i^{CL} values are not dependent or coherent. Avg_{agg}^{CL} and Avg_{pre} are expressed previously in (6) and (7).

$$\min \; MF_{agg}^{CL} = \sqrt{\sum_{i=1}^{61} \sum_{k=0}^{100} (n_i^k \omega_i MF_i^k)^2} \tag{9}$$

$$\text{Subject to:} \; Avg_{agg}^{CL} = Avg_{pre} \pm 0.01 \tag{10}$$

$$\sum_{k=0}^{100} n_i^k = 1, \quad n_i^k \in \{0, 1\} \tag{11}$$

In the same manner with Avg-CL pattern, one of the MF-CL pattern is selected based on the short-term forecasting of weather mode for each region i. Then, $MF_i^k (k = 0 - 100)$ in (9) corresponds to individual plots of the selected MF-CL pattern. By using the constraint in (11), one of the k value

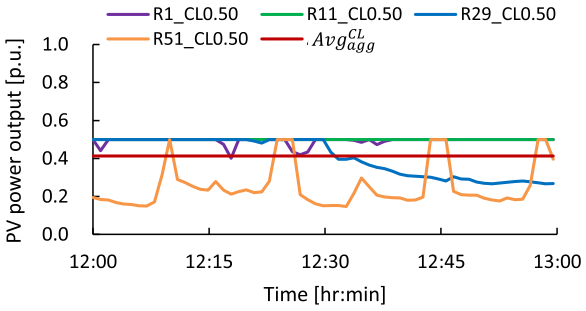

(a) Method-3

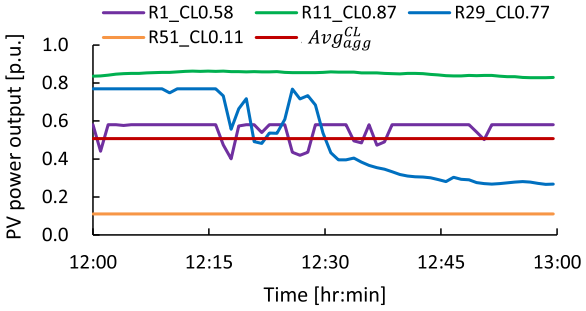

(b) Method-4

FIGURE 10. Application of the comparative methods.

is selected and hence MF_i^k is optimally selected among the 101 candidates.

For the four regions, R1, R11, R29, and R51, the short-term forecast of fluctuations from 12:00 to 13:00 on 1st September provides information that R5 has high MF, R1 has moderate MF, R29 has low MF and R11 has no MF. Hence, they are given the corresponding representative MF-CL patterns that were prepared previously and their patterns are shown in Fig. 8(c).

As a result of the optimization in the case where Avg_{pre} is equal to 0.5 p.u., CL allocated on the four regions are as shown in Fig. 9(b); where R11 of the no MF had the highest CL; R51 of highest MF had a lower CL. The resultant Avg_{agg}^{CL} is 0.53 p.u. and it is close to the Avg_{pre}.

B. COMPARATIVE CL SETTING METHODS

1) METHOD-3

This method allocates the same CL to each region for the actual operation period. For the four regions, R1, R11, R29, and R51, from 12:00 to 13:00 on 1st September, when the Avg_{pre} is 0.5 p.u., the result is as shown in Fig. 10(a). The same CL led to a resultant Avg_{agg}^{CL} of 0.41 p.u. lower than Avg_{pre}, this is because, except for R11, the available output is below 0.5 p.u.

2) METHOD-4

The CL allocation is carried out perfectly using the actual patterns of MF-CL and Avg-CL for the actual operation

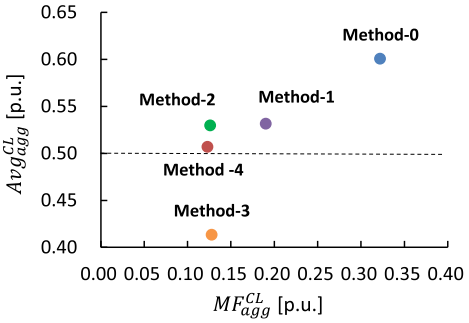

FIGURE 11. MF_{agg}^{CL}- Avg_{agg}^{CL} of all the CL adjustment methods.

period. For the four regions, R1, R11, R29, R51, from 12:00 to 13:00 on 1st September, the actual patterns of Avg-CL and MF-CL as shown in Fig. 6(b) and Fig. 8(b) are used for optimization. The result is shown in Fig. 10(b). The resultant Avg_{agg}^{CL} is 0.51 p.u. and it is extremely close to the Avg_{pre}.

C. COMPARISON OF ALL METHODS FOR THE SAMPLE DAY

When all the methods were applied on the four regions, the resultant Avg_{agg}^{CL} and MF_{agg}^{CL} of each method are plotted in Fig. 11. This gives a general overview on the differences between each method prior to the demonstration of the results of the 61 regions. The summary of the results when the target Avg_{pre} is 0.5 p.u. is as follows:

- Method-0 has the highest deviation from Avg_{agg}^{CL} and the highest MF_{agg}^{CL}. That is when no curtailment is applied at high PV power output, the resultant Avg_{agg}^{CL} deviated from the target Avg_{pre} and fluctuations were not suppressed.
- Method-1 has a very low deviation from Avg_{agg}^{CL} and lower MF_{agg}^{CL} than Method-0. This proposed method focused mainly on reducing the gap between the resultant Avg_{agg}^{CL} and Avg_{pre} along with that fluctuations were reduced.
- Method-2 has a sufficiently low deviation from Avg_{agg}^{CL} and very low MF_{agg}^{CL} that is very close to the ideal Method-4. This proposed method focused on reducing the fluctuations as well as the gap between the resultant Avg_{agg}^{CL} and Avg_{pre}.
- Method-3 has a very high deviation from Avg_{agg}^{CL} and very low MF_{agg}^{CL}. When severe curtailment suppressed the fluctuations, the resultant Avg_{agg}^{CL} majorly deviated from the target Avg_{pre}.
- Method-4 is the closest to Avg_{agg}^{CL} and it has the lowest MF_{agg}^{CL}. Due to the perfect short-term forecasting, the CL was precisely allocated to reduce the fluctuations and achieve the closest resultant Avg_{agg}^{CL} to Avg_{pre}. Despite the perfect forecast used in Method-4, a deviation is witnessed between the resultant Avg_{agg}^{CL} and the Avg_{pre}. This is because CL applied in this method have an

increment of 0.01 p.u. and the actual patterns of MF-CL and Avg-CL are plotted based on this incremental value. To achieve less deviation, less incremental value can be utilized, however, the assumed value of 0.01 p.u. proved to be effective in forming reasonable MF-CL and Avg-CL patterns.

VI. CASE STUDY OF CL ADJUSTMENT USING 61 REGIONS IN CENTRAL JAPAN

In the practical operation, requested Avg_{pre} is set based on the load forecasting for each hour of the next day. In this study, we directly assume different levels of requested Avg_{pre} that indirectly reflects various levels of electricity demand that has to be met by the Avg_{pre} and other generation resources. Thus, we test the effectiveness of the proposed methods at different levels of Avg_{pre} without necessarily deducing the exact electricity demand levels.

In Japan, the four common weather seasons exist, and September is considered to be in the autumn season. The autumn season tends to have many semi-cloudy days, i.e. fluctuating PV power output days. All the methods are applied on all the regions of all days of September at one hour from 12:00 to 13:00. In the proposed method, Avg-CL and MF-CL patterns are prepared for each hour in every month, accordingly for each hour under investigation, the prepared Avg-CL and MF-CL patterns will be used in the operation period. Therefore, for 12:00 to 13:00 in the entire days of September, the previously prepared patterns in Figs. 6(c) and 8(c) will be used. The resulting MF^{CL}_{agg} and Avg^{CL}_{agg} for all the methods are plotted in Fig. 12 at different Avg_{pre} such as 0.7 p.u., 0.5 p.u., and 0.3 p.u.

It is noted that at some data points such as the 12th Sep and 13th Sep, Method-1, Method-2 and Method-4 results are similar to that of Method-0. That happens when the Avg^{CL}_{agg} before CL application is lower than the Avg_{pre}, meaning that there is no adequate PV power output to reach the Avg_{pre} requested in advance. Accordingly, the methods used for adjusting CL in short-term such as Method-1, Method-2 and Method-4 will not be required in such cases, and their output will be similar to Method-0. However, Method-3 where the CL application determined a day-ahead can still apply. Hence, Method-3 seems to be performing the best as it has the lowest MF, however, due to its severe curtailment resultant Avg^{CL}_{agg} becomes the furthest. Apart from these cases, Method-4 is shown to perform that best on days where the short-term CL adjustment is needed.

For the MF^{CL}_{agg} data in Fig. 12, Method-3 mostly has the lowest MF^{CL}_{agg} due to the severe CL applied, while the MF^{CL}_{agg} of Method-0 without CL is always the highest. The MF^{CL}_{agg} of the proposed Method-2 is almost overlapping the ideal Method-4 trends, which proves that Method-2 can replace the usage of Method-4 which is based on challenging perfect forecasting. While, the proposed Method-1 is constantly

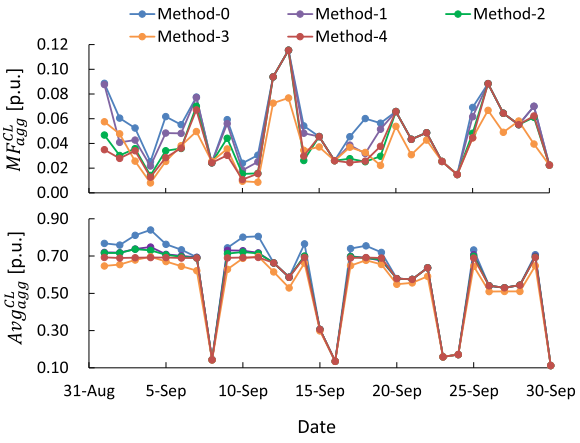

(a) At Avg_{pre} 0.7 p.u.

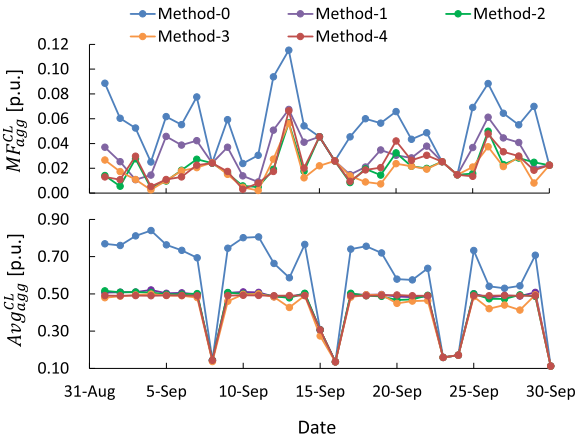

(b) At Avg_{pre} 0.5 p.u.

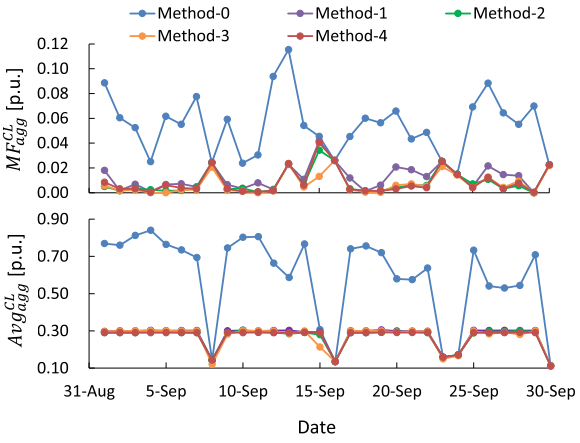

(c) At Avg_{pre} 0.3 p.u.

FIGURE 12. Comparison between all the methods from 12:00 to 13:00 for the 30 days of September 2010.

lower than Method-0, the proposed Method-2 is closer to the ideal Method-4. Since September days are mostly fluctuating, Method-2 suppresses fluctuations along with maintaining the requested Avg_{pre}. Method-1 is less effective than Method-2 at

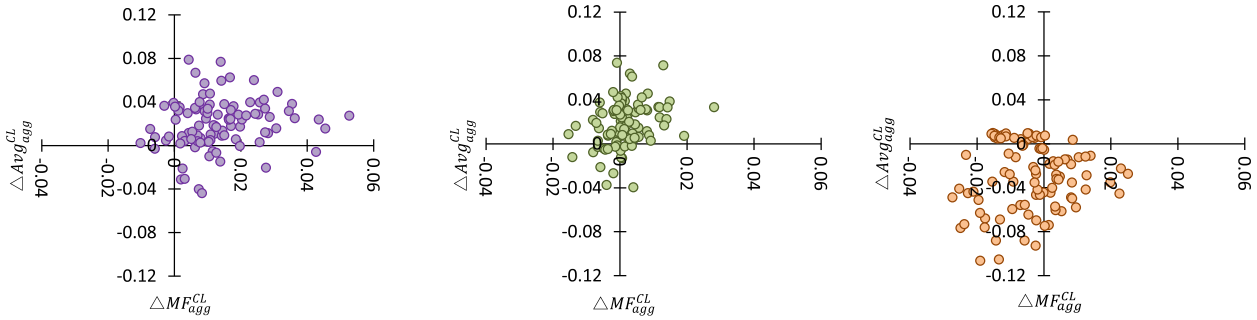

(a) Method-1 and Method-4 (b) Method-2 and Method-4 (c) Method-3 and Method-4

FIGURE 13. Comparison between CL adjustment methods at Avg_{pre} 0.7 p.u. from 12:00 to 13:00 in one year.

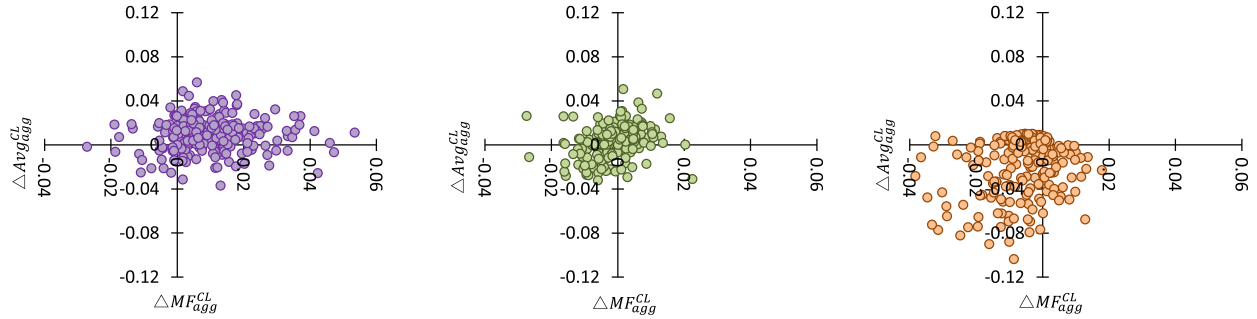

(a) Method-1 and Method-4 (b) Method-2 and Method-4 (c) Method-3 and Method-4

FIGURE 14. Comparison between CL adjustment methods at Avg_{pre} 0.5 p.u. from 12:00 to 13:00 in one year.

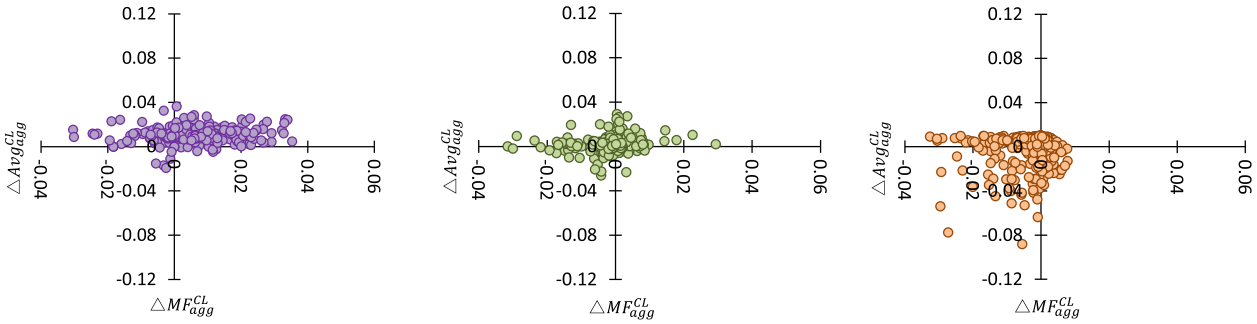

(a) Method-1 and Method-4 (b) Method-2 and Method-4 (c) Method-3 and Method-4

FIGURE 15. Comparison between CL adjustment methods at Avg_{pre} 0.3 p.u. from 12:00 to 13:00 in one year.

higher Avg_{pre} however, the overall MF_{agg}^{CL} is decreased as the Avg_{pre} decreases from 0.7 p.u. to 0.3 p.u.

For the Avg_{agg}^{CL} data in Fig. 12, while the ideal Method-4 always has the closest resultant Avg_{agg}^{CL} to the Avg_{pre}, the least deviation in the other methods is found to be by the proposed methods. The lowest Avg_{agg}^{CL} is Method-3 due to the severe CL applied. As the Avg_{pre} decreases from 0.7 p.u. to 0.3 p.u., the resultant Avg_{agg}^{CL} of all methods except Method-0 are having less deviation from the ideal Method-4.

The proposed methods are evaluated by the difference between the Avg_{agg}^{CL} of the CL adjustment methods respectively and the ideal Method-4 (ΔAvg_{agg}^{CL}). ΔAvg_{agg}^{CL} is plotted against the difference between the MF of the CL adjustment methods respectively and the ideal Method-4 (ΔMF_{agg}^{CL}) in Figs. 13, 14 and 15 for Avg_{pre} of 0.7 p.u., 0.5 p.u., and 0.3 p.u., respectively. The data points in the figures show the relationship between ΔAvg_{agg}^{CL} and ΔMF_{agg}^{CL} for the one hour from 12:00 to 13:00 in the entire year in all the regions. It is noted

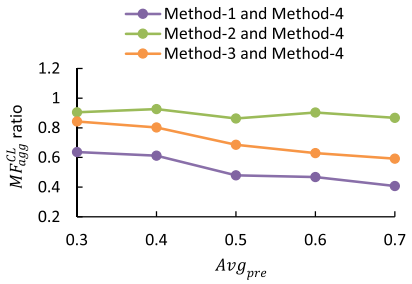

(a) MF^{CL}_{agg} ratio

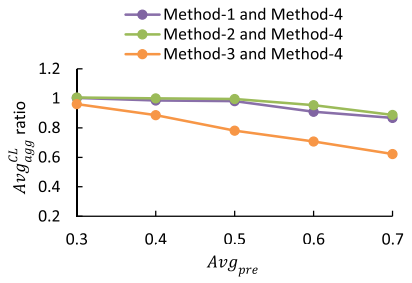

(b) Avg^{CL}_{agg} ratio

FIGURE 16. Ratio of the data points of the resultant ΔMF^{CL}_{agg} and ΔAvg^{CL}_{agg} within a certain threshold, respectively, to the total data points at every Avg_{pre}.

that more data points are found as the Avg^{CL}_{agg} decreases from 0.7 p.u. to 0.3 p.u. This is because the proposed methods are not required when the reliable output before the curtailment is lower than the Avg_{pre}.

Generally, Method-1 has a slightly right-leaning horizontal distribution. This means that Method-1 does not suppress the MF as the ideal Method-4. Method-2 has a distribution centered at the origin, which indicated a small deviation between the proposed method-2 and the ideal Method-4 in terms of both Avg^{CL}_{agg} and MF^{CL}_{agg}. Method-3 has longitudinal distribution, which means that the application of equal CL to all the regions majorly deviates the Avg^{CL}_{agg} from Avg_{pre}.

Therefore, Figs. 13, 14 and 15 indicate that Method-2 can reduce the fluctuations and be close to the ideal Method-4. While centralized data points of Method-1 represent the less fluctuating days that do not necessarily need the operation of Method-2. In Figs. 13, 14 and 15, as the Avg_{pre} decreases from 0.7 p.u. to 0.3 p.u., the data points of the proposed methods, Method-1 and Method-2, become concentrated on a horizontal ellipse centered around the origin because more severe CL is applied. Hence, less MF^{CL}_{agg} is expected and the requested Avg_{pre} is easily reached.

Fig. 16 gives an overview on the resulting ΔMF^{CL}_{agg} and ΔAvg^{CL}_{agg} of each method respectively against the changing Avg_{pre} using the entire data points of the year. Fig. 16 is also used a collective representation of Figs. 13, 14 and 15 including additional results at different Avg_{pre} values. Fig. 16(a) reflects the ratio of the data points that lie within $|\Delta MF^{CL}_{agg}|$ of 0.01 p.u. and the total data points at a certain Avg_{pre} (MF^{CL}_{agg} ratio). Fig. 16(b) reflects the ratio of the data points that lie within $|\Delta Avg^{CL}_{agg}|$ of 0.04 p.u. and the total data points at a certain Avg_{pre} (Avg^{CL}_{agg} ratio).

As the trends of the resulting MF^{CL}_{agg} and Avg^{CL}_{agg} ratios of any method approach 1, it implies that this method is close to ideal Method-4 output. The trends in Fig. 16(a) show that Method-2 is the most efficient at reducing the MF^{CL}_{agg} at any Avg_{pre}. Method-3 shows its efficiency at reducing MF^{CL}_{agg} as the Avg_{pre} decreases, i.e. when severe CL is applied, MF^{CL}_{agg} is reduced drastically. Method-1 is mostly deviated from ideal Method-4 at every Avg_{pre} as reduction of MF^{CL}_{agg} is the least priority of this method and it works the best in non-fluctuating days. The trends in Fig. 16(b) show that Method-1 and Method-2 are the most effective in meeting the target Avg_{pre} at the medium and low Avg_{pre}. In addition, Method-3 has the most deviation from ideal Method-4, however, this deviation reduces as Avg_{pre} decreases, making this method more feasible at low Avg_{pre}.

VII. CONCLUSION

This study proposes methods for the optimal short-term allocation of CL among each region. The allocation of the CL is based on the short-term forecasting of the fluctuation mode of individual PV power output. The proposed method can also reduce the fluctuations in aggregated PV power output.

The proposed method employs two functions, i.e. the relationship between CL and MF, and between CL and Avg prepared for typical fluctuation modes based on statistical data of past solar irradiance observations. Accordingly, the optimal CL is allocated to minimize the fluctuations in aggregated PV power output by merely identifying the region's MF and average modes instead of precisely observing the short-term time-series PV power output.

The proposed methods were tested using the time-series of PV power output at 61 observation points in the central region of Japan for one year. The main results are as follows:

- The proposed methods resulted in optimal CL allocation that majorly reduced MF^{CL}_{agg} and targeted the requested PV output by the operator Avg_{pre}. This will reduce the fluctuations of aggregated PV power output, which contributes to the reduction of the requirement of frequency regulation and required CL of aggregated PV power output itself.
- The results of the proposed methods were found to be almost as effective as the method using perfect short-term forecasting of PV power output. This has been shown through the calculation of the deviation of the proposed methods from the ideal Method-4 and the gaps are manifested to lie within $|\Delta MF^{CL}_{agg}|$ of 0.01 p.u and $|\Delta Avg^{CL}_{agg}|$ of 0.04 p.u.
- The proposed methods becomes functional when there are regions with different modes of power output ranging

from fluctuating to non-fluctuating, and high average to low average regions meaning that different modes of MF-CL and Avg-CL are utilized for optimizing the CL allocation. However, for days with similar modes among different regions, for instance in summer days with high and uniform power output, the same CL application in Method-3 can be sufficient.

Additional study can be conducted to use statistical data for creating more classifications of MF-CL and Avg-CL patterns to reflect more different PV power output behaviors, hence, providing highly accurate CL allocation. Also, by enhancing the short-term forecasting accuracy, more specific MF-CL and Avg-CL patterns can be chosen among the various patterns available.

Another issue which is the interconnection between PV power curtailment and grid congestion can be a potential issue that can investigated in future work. As congestion management can impact PV power curtailment when transmission capacity is limited. Curtailment of some PV systems will then be required to avoid overloading transmission lines.

REFERENCES

[1] R. K. Varma, "Impacts of high penetration of solar PV systems and smart inverter developments," in *Smart Solar PV Inverters With Advanced Grid Support Functionalities*, 1st ed. New York, NY, USA: Wiley, Jun. 2022, pp. 1–34.

[2] M. Patsalides, G. E. Georghiou, A. Stavrou, and V. Efthymiou, "Voltage regulation via photovoltaic (PV) inverters in distribution grids with high PV penetration levels," in *Proc. 8th Medit. Conf. Power Gener., Transmiss., Distribution Energy Convers. (MEDPOWER)*, Oct. 2012, pp. 1–6.

[3] J. Till, S. You, Y. Liu, and P. Du, "Impact of high PV penetration on voltage stability," in *Proc. IEEE/PES Transmiss. Distribution Conf. Expo.*, Oct. 2020, pp. 1–5.

[4] T. Aziz and N. Ketjoy, "PV penetration limits in low voltage networks and voltage variations," *IEEE Access*, vol. 5, pp. 16784–16792, 2017.

[5] S. Shivashankar, S. Mekhilef, H. Mokhlis, and M. Karimi, "Mitigating methods of power fluctuation of photovoltaic (PV) sources—A review," *Renew. Sustain. Energy Rev.*, vol. 59, pp. 1170–1184, Jun. 2016.

[6] D. Kim, H. Kim, and D. Won, "Operation strategy of shared ESS based on power sensitivity analysis to minimize PV curtailment and maximize profit," *IEEE Access*, vol. 8, pp. 197097–197110, 2020.

[7] Y. Singh, B. Singh, and S. Mishra, "An uninterruptable PV array-battery based system operating in different power modes with enhanced power quality," *IEEE Trans. Ind. Electron.*, vol. 69, no. 4, pp. 3631–3642, Apr. 2022.

[8] A. A. Almehizia, H. M. K. Al-Masri, and M. Ehsani, "Integration of renewable energy sources by load shifting and utilizing value storage," *IEEE Trans. Smart Grid*, vol. 10, no. 5, pp. 4974–4984, Sep. 2019.

[9] J. M. Riquelme-Dominguez and S. Martinez, "A photovoltaic power curtailment method for operation on both sides of the power-voltage curve," *Energies*, vol. 13, no. 15, p. 3906, Jul. 2020.

[10] S. Ghosh, S. Rahman, and M. Pipattanasomporn, "Distribution voltage regulation through active power curtailment with PV inverters and solar generation forecasts," *IEEE Trans. Sustain. Energy*, vol. 8, no. 1, pp. 13–22, Jan. 2017.

[11] J. A. Azzolini, M. J. Reno, N. S. Gurule, and K. A. W. Horowitz, "Evaluating distributed PV curtailment using quasi-static time-series simulations," *IEEE Open Access J. Power Energy*, vol. 8, pp. 365–376, 2021.

[12] M. Z. Liu, A. T. Procopiou, K. Petrou, L. F. Ochoa, T. Langstaff, J. Harding, and J. Theunissen, "On the fairness of PV curtailment schemes in residential distribution networks," *IEEE Trans. Smart Grid*, vol. 11, no. 5, pp. 4502–4512, Sep. 2020.

[13] M. Zeraati, M. E. H. Golshan, and J. M. Guerrero, "A consensus-based cooperative control of PEV battery and PV active power curtailment for voltage regulation in distribution networks," *IEEE Trans. Smart Grid*, vol. 10, no. 1, pp. 670–680, Jan. 2019.

[14] R. Lopes and M. Paolene, "PV curtailment for managing the variability of solar power generation: A review of current practices and emerging solutions," *IEEE Trans. Sustain. Energy*, vol. 11, no. 4, pp. 2284–2294, Oct. 2020.

[15] Kyushu Electric Power Transmission and Distribution. *Publication of Grid Information*. Accessed: Apr. 20, 2023. [Online]. Available: https://www.kyuden.co.jp/td_service_wheeling_rule-document_disclosure

[16] E. Ekomwenrenren, Z. Tang, J. W. Simpson-Porco, E. Farantatos, M. Patel, and H. Hooshyar, "Hierarchical coordinated fast frequency control using inverter-based resources," *IEEE Trans. Power Syst.*, vol. 36, no. 6, pp. 4992–5005, Nov. 2021.

[17] L. Montero, A. Bello, and J. Reneses, "A review on the unit commitment problem: Approaches, techniques, and resolution methods," *Energies*, vol. 15, no. 4, p. 1296, Feb. 2022.

[18] H. Sangrody, N. Zhou, and Z. Zhang, "Similarity-based models for day-ahead solar PV generation forecasting," *IEEE Access*, vol. 8, pp. 104469–104478, 2020.

[19] B. Lu and M. Shahidehpour, "Unit commitment with flexible generating units," *IEEE Trans. Power Syst.*, vol. 20, no. 2, pp. 1022–1034, May 2005.

[20] Y. Udagawa, Y. Nishitsuji, K. Ogimoto, J. G. S. Fonseca, H. Ohtake, T. Oozeki, T. Ikegami, and S. Fukutome, "Analysis of photovoltaic power yield curtailment in day-ahead unit commitment," *IEEJ Trans. Power Energy*, vol. 137, no. 7, pp. 520–529, 2017.

[21] T. Masuta, D. Kobayashi, H. Ohtake, and N. H. Viet, "Evaluation of unit commitment based on intraday few-hours-ahead photovoltaic generation forecasts to reduce the supply-demand imbalance," in *Proc. 8th Int. Renew. Energy Congr. (IREC)*, Mar. 2017, pp. 1–5.

[22] U. K. Das, K. S. Tey, M. Seyedmahmoudian, S. Mekhilef, M. Y. I. Idris, W. Van Deventer, B. Horan, and A. Stojcevski, "Forecasting of photovoltaic power generation and model optimization: A review," *Renew. Sustain. Energy Rev.*, vol. 81, pp. 912–928, Jan. 2018.

[23] L. Gigoni, A. Betti, E. Crisostomi, A. Franco, M. Tucci, F. Bizzarri, and D. Mucci, "Day-ahead hourly forecasting of power generation from photovoltaic plants," *IEEE Trans. Sustain. Energy*, vol. 9, no. 2, pp. 831–842, Apr. 2018.

[24] E. Lorenz, J. Hurka, D. Heinemann, and H. G. Beyer, "Irradiance forecasting for the power prediction of grid-connected photovoltaic systems," *IEEE J. Sel. Topics Appl. Earth Observ. Remote Sens.*, vol. 2, no. 1, pp. 2–10, Mar. 2009.

[25] J.-H. Kim, P. A. J. Munoz, M. Sengupta, J. Yang, J. Dudhia, S. Alessandrini, and Y. Xie, "The WRF-solar ensemble prediction system to provide solar irradiance probabilistic forecasts," *IEEE J. Photovolt.*, vol. 12, no. 1, pp. 141–144, Jan. 2022.

[26] J. Shi, W.-J. Lee, Y. Liu, Y. Yang, and P. Wang, "Forecasting power output of photovoltaic systems based on weather classification and support vector machines," *IEEE Trans. Ind. Appl.*, vol. 48, no. 3, pp. 1064–1069, May 2012.

[27] H.-T. Yang, C.-M. Huang, Y.-C. Huang, and Y.-S. Pai, "A weather-based hybrid method for 1-day ahead hourly forecasting of PV power output," *IEEE Trans. Sustain. Energy*, vol. 5, no. 3, pp. 917–926, Jul. 2014.

[28] I. Kaaya and J. Ascencio-Vasquez, "Photovoltaic power forecasting methods," in *Solar Radiation—Measurement, Modeling and Forecasting Techniques for Photovoltaic Solar Energy Applications*. London, U.K.: Intech, Apr. 2021. [Online]. Available: https://www.intechopen.com/chapters/76055

[29] W. Hu, X. Zhang, L. Zhu, and Z. Li, "Short-term photovoltaic power prediction based on similar days and improved SOA-DBN model," *IEEE Access*, vol. 9, pp. 1958–1971, 2021.

[30] J. Yan, L. Hu, Z. Zhen, F. Wang, G. Qiu, Y. Li, L. Yao, M. Shafie-Khah, and J. P. S. Catalão, "Frequency-domain decomposition and deep learning based solar PV power ultra-short-term forecasting model," *IEEE Trans. Ind. Appl.*, vol. 57, no. 4, pp. 3282–3295, Jul. 2021.

[31] Z. Zhen, J. Liu, Z. Zhang, F. Wang, H. Chai, Y. Yu, X. Lu, T. Wang, and Y. Lin, "Deep learning based surface irradiance mapping model for solar PV power forecasting using sky image," *IEEE Trans. Ind. Appl.*, vol. 56, no. 4, pp. 3385–3396, Jul. 2020.

[32] M. S. Hossain and H. Mahmood, "Short-term photovoltaic power forecasting using an LSTM neural network and synthetic weather forecast," *IEEE Access*, vol. 8, pp. 172524–172533, 2020.

[33] C.-J. Huang and P.-H. Kuo, "Multiple-input deep convolutional neural network model for short-term photovoltaic power forecasting," *IEEE Access*, vol. 7, pp. 74822–74834, 2019.

[34] B. D. Dimd, S. Völler, U. Cali, and O.-M. Midtgard, "A review of machine learning-based photovoltaic output power forecasting: Nordic context," *IEEE Access*, vol. 10, pp. 26404–26425, 2022.

[35] T. Kato, T. Murase, M. Kurimoto, Y. Manabe, and T. Funabashi, "Modelling of aggregated power output of photovoltaic power generation in consideration of smoothing effect of power output fluctuation around observation point," *Renew. Energy Power Quality J.*, vol. 1, pp. 456–461, Apr. 2018.

NOHA HARAG received the B.Sc. degree in renewable energy engineering from the University of Science and Technology, Zewail City, Egypt, in 2018, and the M.Sc. degree in electrical engineering from Nagoya University, Nagoya, Japan, in 2020, where she is currently pursuing the Ph.D. degree in electrical engineering. Her research interests include control solutions to integrated energy systems and power system dynamics.

CHIYORI T. URABE (Member, IEEE) received the B.Sc. and M.Sc. degrees in nonlinear physics from Nara Women's University, Japan, in 1998 and 2000, respectively, and the Ph.D. degree in non-equilibrium statistical physics from Kyoto University, Japan, in 2006. She was a Researcher with Osaka University, Meiji University, and Japan Science and Technology Agency. From 2013 to 2022, she was a Project Assistant Professor with Tokyo University, Japan. Since 2022, she has been an Assistant Professor with Nagoya University, Japan. Her research interests include renewable energy and energy system integration.

TAKEYOSHI KATO (Member, IEEE) received the B.Sc., M.Sc., and Ph.D. degrees in electrical engineering from Nagoya University, Nagoya, Japan, in 1991, 1993, and 1996, respectively. From 1996 to 2015, he was the Faculty Member of Nagoya University, where he has been a Professor, since 2015. His research interests include the modeling/forecasting of electricity demand and renewable power output, the control and planning of electric power systems, and the integration of renewable energy with urban design.